RSC Advances

ROYAL SOCIETY OF CHEMISTRY

www.rsc.org/advances

Cite this: DOI: 10.1039/c0xx00000x

www.rsc.org/xxxxxx

ARTICLE TYPE

Tuning the electrochemical performances of anthraquinoneorganic cathode materials for Li-ion batteries through the sulfonic sodium functional group

Wang Wan,[a] Hungsui Lee,[b] Xiqian Yu, *[b] Chao Wang, [a] Kyung-wan Nam, [b] Xiao-Qing Yang*[b] and Henghui Zhou*[a]

Received (in XXX, XXX) XthXXXXXXXXX 20XX, Accepted Xth XXXXXXXXX 20XX
DOI: 10.1039/b000000x

The effectson electrochemical performance of $C_{14}H_8O_2$ organic cathode materials with and without SO_3Na-functional groups for lithium ion batteries were investigated. The $Na_2C_{14}H_6O_8S_2$ with two SO_3Na- shows the best cycle performance and highest lithium storage voltage, while an outstanding rate performance is also achieved after combined with graphene paper.

Based on the low cost, environmental friendly nature, and great varieties of chemical compounds in a wide potential range, developing organic compounds for electrode materials has attracted a lot of attentions from rechargeable battery research. A large number of electroactive organic compounds have been studied.[1-11] Among them, quinonebased compounds areespecially interesting. It has been reported that quinone can be used as cathode materials for lithium ion batteries.[9, 12-17] With a suitable lithium storage potential in a range between 2 to 3 V vs. Li/Li^+. However, like most other organic electrode materials[8, 18, 19], quinone also suffers from poor cycle performance, which is mainly due to its high solubility in electrolytes.[16]

A lot of efforts have been made toresolve the dissolution issue of the organic electrode materials. Polymerization is one of the most effective approaches being widely used and reported in the literatures. Song et al. synthesized a poly (anthraquinone sulfide) which showed excellent reversibility and cyclability.[20] Wei et al. reported a polyimide/CNT composite showing a good cycle stability of up to 93% of the initial capacity after 300 cycles[8]. Grafting the organic molecules on the insoluble substrates is another effective approach to suppress the dissolution of the organic materials. Genorio et al. immobilized quinone derivative materials by grafting them onto SiO_2 nanoparticles and carbon black. Relying on the covalent grafting and electrochemical grafting, the quinone derivatives are quite stable during the entire cycling process.[3, 16] This method improved the cycle stability significantly, but sacrificed a large amount of the specific capacity of electrode materials. Recently, Zeng et al. reported a new anthraquinone derivate, $Li_2(C_{14}H_6O_4)$, which can greatly inhibit the dissolution of the anthraquinone into electrolyte resulting in good cycle performance.[21] However, although the dissolution of anthraquinone was reduced by adding lithia functional group (LiO-), the average lithium storage voltage was lowered, which is undesirable for cathode application.

Certain redox active centers of organic molecules (and also polymers) offer various combinations of atomic arrangements and functional group substitutions which may provide capabilities for fine tuning their properties to the desirable performance.[3, 19, 22-25] Therefore, introducing functional groups to the quinone molecule will not only open a new approach to solve the dissolution problems of organic cathode materials, but also provide valuable guidance for tuning other properties such as specific capacity and lithium storage potential. In this paper, we reported a series of sodium functional groups (SO_3Na-) modified anthraquinone ($C_{14}H_8O_2$, AQ) compounds and studied the effects of these functional groups on the electrochemical properties of these compounds as cathode materials for Li-ion batteries. Since the specific capacity will decrease with increasing number of the SO_3Na- function groups per anthraquinone, the highest number of this functional group is limited to two and only anthraquinone-1-sulfonic acid sodium ($NaC_{14}H_7O_5S$, AQS) and anthraquinone-1,5-disulfonic acid sodium ($Na_2C_{14}H_6O_8S_2$, AQDS) salts were studied in comparison with no modified AQ in this work. It will be shown later in this paper that the interionic and/or intermolecular forces between sulfonic groups can suppress the dissolution of the modified anthraquinone compounds in electrolyte, resulting in a significant improvement of the cycle performance. In addition, a higher lithium storage voltage can be achieved through sulfonic modification, attributed to the electron withdrawing function of the sulfonic group.

Thermal stability is one important factor of the electrode materials which may influence their further modification.[26] Therefore the thermal stability of these three compounds was evaluated first by thermogravimetric (TG) analysis under nitrogen atmosphere. It can be seen in Fig. S1 that the onset decomposition temperatures of AQ, AQS and AQDS (with 0, 1 and 2 SO_3Na- group) are around 250, 440 and 520 ℃, respectively, indicating the increased thermal stability of the anthraquinone compounds by adding SO_3Na- functional group, and AQDS shows the best thermal stability.

The investigated anthraquinone compounds are well crystallized as can be proved by the XRD patterns shown in Fig. S2. SEM images were used to examine the morphology of these three compounds and the results are shown in the inserted images

in Fig. 1b (A, B, C). It can be seen that the morphology of these three compounds are almost the same with particle size distributed in micron meter level. Therefore, the electrochemical performance of these three compounds is not much influenced by the morphology differences of these samples. Fig. 1a plotted the charge-discharge profiles of these three compounds recorded at a current density of 0.1 C-rate in the voltage range of 1.5 V-4 V. It is interesting to note that the Li storage voltage of these compounds is strongly affected by the sulfonic sodium functional group. The AQDS with two sulfonic sodium groups at the 1, 5 sites of the AQ shows the highest lithium storage voltage at around 2.4 V, while the unmodified AQ shows the lowest average storage voltage at around 2.1 V. AQS has an average lithium storage voltage at around 2.25 V, which is between AQDS and AQ, indicating that after adding SO_3Na- functional group, the lithium storage voltage has been improved, which can be attributed to the electron withdrawing effect of SO_3Na- functional group. The electron withdrawing effect will reduce the electron density of carbon atoms nearby. Owning to the conjugated effect on the ring, there is also a strong effect on the carbonyl groups, thereby the electron density of the carbonyl groups is reduced while the oxidizability is enhanced. As a result, redox potential has been improved.[27] The cyclic voltammetry (CV) curves of AQS and AQDS which are given in Fig. S3. Both of them show two pairs of redox peaks which are similar to the result reproted by Zeng et al,[21] indicating a two-step reaction lithium storage mechanism.

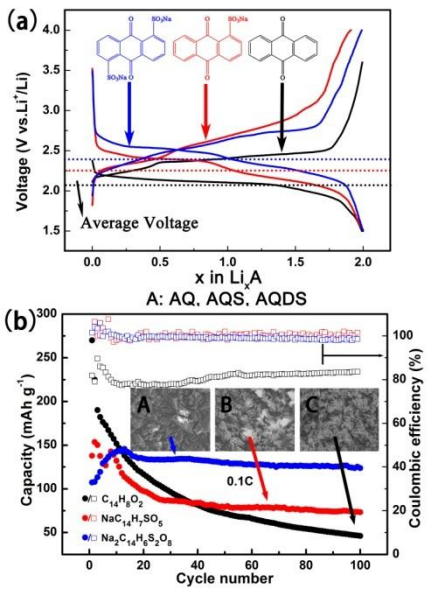

Fig. 1 Typical (a) charge and discharge curves and (b) cycle performance and coulombic efficiency of AQ, AQS, and AQDS electrodes cycled at 0.1 C-rate. The inset pictures are the SEM images of these three compounds.

The cycle performance of these three compounds are investigated under 0.1 C-rate charge/discharge (Fig. 1b). The theoretical capacities of these three materials are provided in Table. S1. It's obvious that after modifying anthraquinone with SO_3Na- functional group, the cycle performance is significantly improved. The AQDS shows the best cycle performance. No obvious capacity fading can be observed during cyclingand a reversible specific capacity of 120 mAh g^{-1} can be retained after 100 cycles. For AQ with no SO_3Na- functional group, although it shows the highest initial discharge capacity of around 270 mAh g^{-1}, continued severe capacity fading is observed in subsequent cycling. A reversible capacity of only 40 mAh g^{-1} can be generated after 100 cycles. AQS with one SO_3Na- functional group shows a higher specific capacity than AQDS at the first cycle, which is consistent with the trend shown in table S1, and it shows a cycle performance poorer than AQDS but better than AQ. We can also see that the coulombic efficiency of AQ is the lowest, ca. 80%, which is mainly due to the dissolution of AQ during the charge and discharge process. The coulombic efficency of the AQS and AQDS is around 100%.

The improved cycle performance by adding SO_3Na- functional group can be attributed to the decreased compound dissolution into electrolyte, as shown by the ultraviolet (UV) spectroscopy analysis (Fig. S4). When collecting the UV spectra, AQ, AQS and AQDS were dissolved in DMC solvent and the solutions were examined by UV spectroscopy respectively. It can be seen that AQ/DMC solution shows a large absorption peak at around 350 cm^{-1}, indicating a large amount of AQ can be dissolved into DMC solvent. After adding one SO_3Na- functional group to form AQS, its solubility is greatly reduced. The AQDS with two SO_3Na- functional groups shows the lowest solubility, as evidenced on the UV spectrum where the absorption peak assigned to AQDS is very weak.

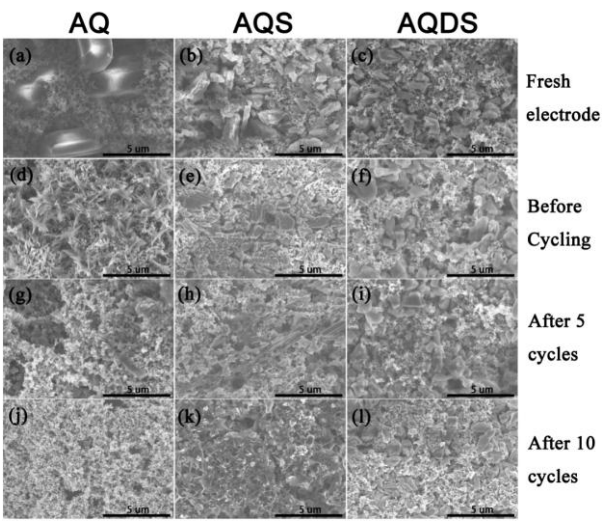

Fig. 2 SEM of AQ, AQS, and AQDS electrodes: fresh electrode (a), (b), (c) before cycling (d), (e), (f) after 5 cycles (g), (h), (f) after 10 cycles (j), (k), (l), respectively.

The morphology changes of the electrodes after cycling were further examined by SEM to see the dissolution effects of these three compounds. Fig. 2 shows the SEM images the fresh electrodes of AQ, AQS, and AQDS, and the electrodes before and after cycling at a current rate of 0.1 C. Fresh electrodes were examined directly, and all the other electrodes are made into cells and keep in the cells with the same time of about 10 days, containing the cycling time. It can be seen from Fig. 2a, b, and c that the compounds in fresh electrodes are distributed uniformly in the electrodes with a particle size in micrometer. It is obvious from Fig. 2d that the morphology of the AQ electrode has changed a lot after placing in the coin cells for 10 days. The

original blocks disappeared and some dendrite like crystal formed, indicating that AQ has dissolved into the electrolyte. The morphology of AQS electrode after 10 days' storage in cells has a few changes (Fig. 2e). Some particles become smaller which is also due to the dissolution of AQS in electrolyte. However, the morphology of AQDS electrodes with two SO_3Na- groups remains almost the same as the fresh electrode after holding in cell for 10 days (Fig. 2f), indicating that the dissolution of AQDS compound into electrolyte is much less than AQS and AQ. It can also be approved by the morphology change of electrodes with cycling in Fig. 2g-l. It is obvious that after 5 cycles of AQ electrode, there are some holes appearing on the electrode and the AQ particles become smaller and less, indicating that most of AQ are dissolved into electrolyte. After 10 cycles, nearly no AQ particles can be observed. We can conclud that the dissolution speed can be quickened by the charge and discharge processes in coin cells. Dissolution phenomena of AQS electrode after cycling has been improved very much from AQ, but the morphology of AQDS electrodes keeps nearly the same even after cycled for 10 times, further indicating that AQDS compound has the lowest solubility in electrolyte. It is clear that after adding SO_3Na-functional group, the dissolution phenomena is partially suppressed, and AQDS shows the best stability in electrolyte.

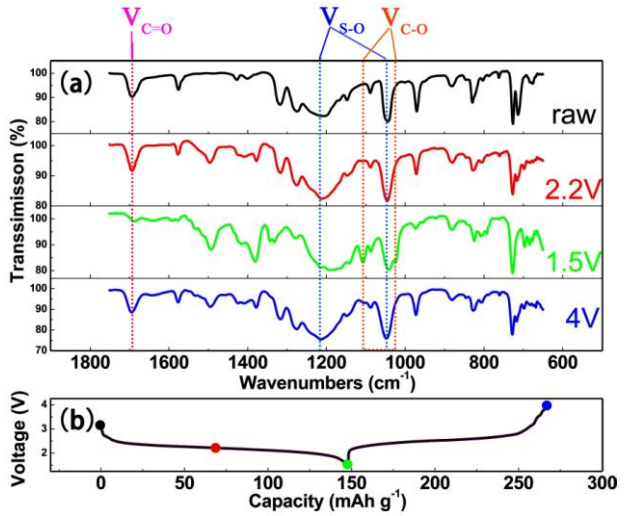

Fig. 3 FTIR spectra of AQDS compound at different charge and discharge stages as marked on the charge-discharge curve.

It has been reported that the lithium storage mechanism (schematically shown in Fig. S5) of AQ is a transition between anthraquinone and anthranol salt.[5, 15] Whether it remains the same after SO_3Na- modification was further studied through Fourier transformed infrared (FTIR) spectroscopy analysis. Fig. 3 shows the FTIR spectra of the half-discharged (red), fully discharged (green) and recharged (blue) AQDS were collected along with the pristine AQDS (black). It can be concluded that the reaction center is still on the carbonyl group, as can be seen that the peak pertaining to the C=O vibration (1695 cm^{-1}) disappeared while the C-O vibration peaks (1020 cm^{-1} and 1105 cm^{-1}) appeared upon discharging. The peaks centered at 1215 cm^{-1} and 1145 cm^{-1} are associated with the vibration of the sulfonic group. These peaks only show a slight position shift which may becaused by the change of molecular structure from anthraquinone to anthranol after discharge. This indicates the SO_3Na- functional groups do not participate in the reaction. Therefore it can be conclude that the higher the number of SO_3Na- functional groups linked on AQ, the smaller the specific capacity it will be delivered. The lithium storage mechanism of the AQDS compound during charge and discharge can be describes in the following equation:

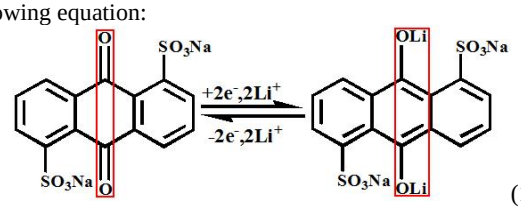

(1)

This reaction is highly reversible, which can be proved by the similar FTIR features of the pristine and recharged AQDS shown in Fig. 3.

Since the AQDS exhibits excellent cycle performance, the rate capability was also examined under various C-rates at 0.2, 0.5, 1, 2, 3, 5 and 10 C.The rate performance of the AQDS is not too good with specific capacities of about 130, 110 and 90 mAh g^{-1} at 0.2 C, 0.5C, and 1 C, respectively (as shown in Fig. 4). When the rate increased to 5 C, only 30 mAh g^{-1} reversible capacity can be obtained. The AQDS shows nearly no reversible capacity when the current densityis up to 10 C. The poor rate capability is mainly cause by the poor electronic conductivity of this organic material, which is a common problem for most organic electrode materials.[28] The reversible lithium storage behavior at 0.2 C can be recovered to 125 mAh g^{-1}after high rate cycling at 10 C, further indicating a good structural stability of AQDS.

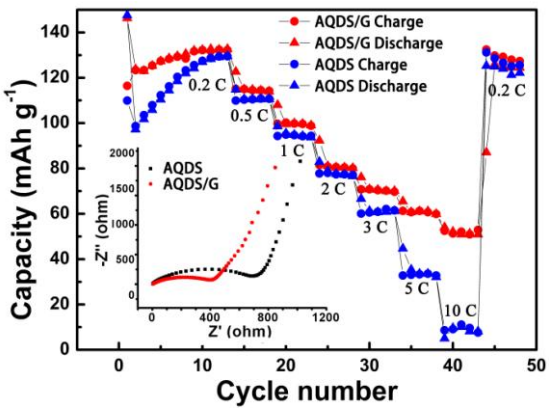

Fig. 4 Rate performance of AQDS and AQDS/G paper electrodes. The inset figure shows the Nyquist plots ofAQDS and AQDS/G paper electrodes.

In order to improve the rate performance of AQDS compound, graphene as a most effective material to improve the electronic conductivity is applied. An effective and facile approach has been explored to synthesis the AQDS and graphene paper composite (AQDS/G paper). It can be seen from the SEM images (Fig. 5 (a) and (b)) that the AQDS particles were uniformly dispersed on the graphene paper. The as-prepared AQDS/G paper discs as shown in Fig. 5 (c) were directly used as electrodes to evaluate the rate capability. The rate performances are provided in Fig. 4 and the corresponding charge-discharge curves at different rates are shown in Fig. S6. It is obvious that AQDS/G paper has a much better rate performance in comparison with pure AQDS. The

specific discharge capacities are around 130, 110, 100, 80, 70, 60 mAh g^{-1} at 0.2, 0.5, 1, 2, 3, and 5 C rates, respectively. A reversible capacity of 50 mAh g^{-1} can be obtained even cycled at rate as high as 10 C rate. The corresponding charge-discharge curves at different C-rate can be seen in Fig. S6.

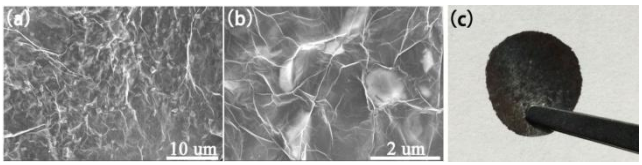

Fig. 5 The SEM images (a)(b) and photo (c) of the AQDS/G paper.

Electrochemical impedance spectroscopy (EIS) experiments were performed to explain the superior rate performances of the AQDS/G paper (inset figure 4). The Nyquist plots ofboth AQDS and AQDS/G paper electrodes before cycling are inserted in Fig. 4. It is clearly that the AQDS/G paper electrode exhibits a much lower charge transfer resistance than the pure AQDS eletrode, which can be attributed to the enhanced conductivity of the AQDS/G paper. The equivalent circuit model was used to fit the Nyquist plots, and the fitted impedance parameters are listed in Fig. S7. The pure AQDS electrode shows an R_{ct} of 740 Ω, much larger than that of AQDS/G paper electrode, which is only 438 Ω. This confirms that the incorporation of the graphene paper can greatly enhance the conductivity AQDS and hence expedite the electron transport during the electrochemical lithium insertion/extraction reaction, leading to significant improved electrochemical performances.

Conclusions

In summary, the effects of the SO_3Na- functional groups on the electrochemistry performances of the anthraquinone compounds were studied. It was found that the SO_3Na- is electrochemically inactive during electrochemical process. Therefore, the specific capacity of the anthraquinone compounds decreases when increasing the number of the SO_3Na- group. On the other hand, the structural stability and the electrochemical cycle performance are significantly improved, due to the inorganic feature of the SO_3Na- group. The anthraquinone with two SO_3Na- functional groups (AQDS) achieves excellent cycle performance as well as moderate reversible capacity. In addition, the average lithium storage voltage increases with increasing number of SO_3Na- groups. The SO_3Na- modification plays multi-functional roles both in solving the dissolution problem of the anthraquinone compounds into electrolytes and in tuning the lithium storage voltage. These results will provide valuable guidance in designing other organic electrode materials. Furthermore, AQDS/Graphene paper electrode was synthesized through a simple and efficient method, which can significantly improve the electronic conductivity of the electrodes and greatly benefit the rate capability. It will provide a facile approach to optimize the electrochemical performance of the organic electrode materials.

We appreciate the financial support from the A*Star Singapore-China Joint Research Program (no. 2012DFG52130). This work at BNL was supported by the U.S. Department of Energy, the Assistant Secretary for Energy Efficiency and Renewable Energy, Office of Vehicle Technologies under Contract Number DEAC02-98CH10886. The support provided by China Scholarship Council (CSC) during a visit of Wang Wan to Brookhaven National Lab is acknowledged. The authors acknowledge technical supports by the beamline scientist Dr. Jianming Bai at X14A (NSLS, BNL)

Notes and references

[a]*College of Chemistry and Molecular Engineering, Peking University, Beijing, P. R. China. Fax: 86-10-62754680; Tel: 86-10-62754680; E-mail: hhzhou@pku.edu.cn.*
[b]*Brookhaven National Laboratory, Upton, New York 11973, USA, Tel: 1-631-3443663; E-mail: xyu@bnl.gov, xyang@bnl.gov.*

†Electronic Supplementary Information (ESI) available: experiment details of making graphene oxide, table of the general properties of AQ, AQS and AQDS, XRD patterns, CV curves UV spectra, charge-discharge curves and equivalent circuit model of the corresponding Nyquist plots. See DOI: 10.1039/b000000x/

1. X. Han, C. Chang, L. Yuan, T. Sun and J. Sun, *Adv. Mater.*, 2007, 19, 1616-1621.
2. M. Armand, S. Grugeon, H. Vezin, S. Laruelle, P. Ribiere, P. Poizot and J. M. Tarascon, *Nat. Mater.*, 2009, 8, 120-125.
3. B. Genorio, K. Pirnat, R. Cerc Korosec, R. Dominko and M. Gaberscek, *Angew. Chem. Int. Ed.*, 2010, 49, 7222-7224.
4. P. Poizot and F. Dolhem, *Energy Environ. Sci.*, 2011, 4, 2003-2019.
5. Y. Liang, Z. Tao and J. Chen, *Adv. Energy Mater.*, 2012, 2, 742-769.
6. S. Renault, D. Brandell, T. Gustafsson and K. Edstrom, *Chem. Commun.*, 2013, 49, 1945-1947.
7. L. Zhao, J. Zhao, Y. Hu, H. Li, Z. Zhou, M. Armand and L. Chen, *Adv. Energy Mater.*, 2012, 2, 962-965.
8. Z. Wei, H. Wu, K. Wang, Y. Meng and K. Lu, *J. Mater. Chem. A*, 2013.
9. W. Xu, A. Read, P. K. Koech, D. Hu, C. Wang, J. Xiao, A. B. Padmaperuma, G. L. Graff, J. Liu and J. Zhang, *J. Mater. Chem.*, 2012, 22, 4032-4039.
10. Z. Song, H. Zhan and Y. Zhou, *Angew. Chem. Int. Ed.*, 2010, 49, 8444-8448.
11. C. Luo, Y. Zhu, Y. Xu, Y. Liu, T. Gao, J. Wang and C. Wang, *J. Power Sources*, 2014, 250, 372-378.
12. Y. Liang, P. Zhang and J. Chen, *Chem. Sci.*, 2013, 4, 1330-1337.
13. Z. Lei, W. Weikun, W. Anbang, Y. Zhongbao, C. Shi and Y. Yusheng, *J. Electrochem. Soc.*, 2011, 158, A991.
14. H. Chen, M. Armand, M. Courty, M. Jiang, C. P. Grey, F. Dolhem, J. M. Tarascon and P. Poizot, *J. Am. Chem. Soc.*, 2009, 131, 8984-8988.
15. L. Zhao, W. Wang, A. Wang, K. Yuan, S. Chen and Y. Yang, *J. Power Sources*, 2013, 233, 23-27.
16. K. Pirnat, R. Dominko, R. Cerc Korosec, G. Mali, B. Genorio and M. Gaberscek, *J. Power Sources*, 2012, 199, 308-314.
17. C. Luo, R. Huang, R. Kevorkyants, M. Pavanello, H. He and C. Wang, *Nano Lett.*, 2014, 14, 1596-1602.
18. L. Zhan, Z. Song, N. Shan, J. Zhang, J. Tang, H. Zhan, Y. Zhou, Z. Li and C. Zhan, *J. Power Sources*, 2009, 193, 859-863.
19. T. Nokami, T. Matsuo, Y. Inatomi, N. Hojo, T. Tsukagoshi, H. Yoshizawa, A. Shimizu, H. Kuramoto, K. Komae, H. Tsuyama and J. Yoshida, *J. Am. Chem. Soc.*, 2012, 134, 19694-19700.
20. Z. Song, H. Zhan and Y. Zhou, *Chem. Commun.*, 2009, 0, 448-450.
21. R. Zeng, X. Li, Y. Qiu, W. Li, J. Yi, D. Lu, C. Tan and M. Xu, *Electrochem. Commun.*, 2010, 12, 1253-1256.
22. J. Geng, J. P. Bonnet, S. Renault, F. Dolhem and P. Poizot, *Energy Environ. Sci.*, 2010, 3, 1929-1933.
23. D. J. Kim, S. H. Je, S. Sampath, J. W. Choi and A. Coskun, *RSC Adv.*, 2012, 2, 7968-7970.
24. S. E. Burkhardt, J. Bois, J. M. Tarascon, R. G. Hennig and H. D. Abruña, *Chem. Mater.*, 2012, 25, 132-141.
25. S. Wang, L. Wang, K. Zhang, Z. Zhu, Z. Tao and J. Chen, *Nano Lett.*, 2013, 13, 4404-4409.
26. M. Armand and J. M. Tarascon, *Nature*, 2008, 451, 652-657.

27. L. F. Fieser and M. Fieser, *J. Am. Chem. Soc.*, 1935, 57, 491-494.
28. W. Walker, S. Grugeon, O. Mentre, S. Laruelle, J. M. Tarascon and F. Wudl, *J. Am. Chem. Soc.*, 2010, 132, 6517-6523.